ChemPubSoc Europe

DOI: 10.1002/cssc.201700409

CHEMSUSCHEM Full Papers

Coatable Li_4SnS_4 Solid Electrolytes Prepared from Aqueous Solutions for All-Solid-State Lithium-Ion Batteries

Young Eun Choi[+],[a] Kern Ho Park[+],[a] Dong Hyeon Kim,[a] Dae Yang Oh,[a] Hi Ram Kwak,[a] Young-Gi Lee,[b] and Yoon Seok Jung*[a]

Bulk-type all-solid-state lithium-ion batteries (ASLBs) for large-scale energy-storage applications have emerged as a promising alternative to conventional lithium-ion batteries (LIBs) owing to their superior safety. However, the electrochemical performance of bulk-type ASLBs is critically limited by the low ionic conductivity of solid electrolytes (SEs) and poor ionic contact between the active materials and SEs. Herein, highly conductive (0.14 mS cm^{-1}) and dry-air-stable SEs (Li_4SnS_4) are reported, which are prepared using a scalable aqueous-solution process. An active material ($LiCoO_2$) coated by solidified Li_4SnS_4 from aqueous solutions results in a significant improvement in the electrochemical performance of ASLBs. Side-effects of the exposure of $LiCoO_2$ to aqueous solutions are minimized by using predissolved Li_4SnS_4 solution.

Introduction

Lithium-ion batteries (LIBs) are commonly used in small-scale applications, but in recent years they have also become increasingly important for large-scale applications such as electric vehicles (EVs).[1] However, safety concerns with LIBs, originating from their use of flammable organic liquid electrolytes, have hindered their widespread commercial application. Accordingly, composite-structured bulk-type all-solid-state lithium-ion batteries (ASLBs) using inorganic solid electrolytes (SEs) have emerged as promising alternatives.[2] To achieve performance levels in bulk-type ASLBs that compete with those of conventional LIBs, development of highly conductive SEs is imperative.[2a,b,e,3] Several sulfide SEs exhibit extremely high conductivities (e.g., $Li_{10}GeP_2S_{12}$: 12 mS cm^{-1},[2a] $Li_3P_7S_{11}$: 17 mS cm^{-1},[3a] $Li_{9.54}Si_{1.74}P_{1.44}S_{11.7}Cl_{0.3}$: 25 mS cm^{-1}[2e]) that are comparable to those of organic liquid electrolytes.[4] Considering that SEs are single ionic conductors, whereas transference numbers for Li^+ ions in organic liquid electrolytes are low (0.2–0.4),[2b,e,4] ASLBs employing state-of-the-art sulfide SEs may, in theory, outperform conventional LIBs.

Another critical challenge with bulk-type ASLBs is to achieve favorable interfaces between the active material and the SE. High interfacial resistances are observed between sulfide SEs and conventional cathode materials such as $LiCoO_2$. This can be explained by the intrinsically poor oxidation stability of sulfide materials,[5] chemical reactions between sulfide SEs and active materials,[5,6] the space-charge-layer model,[7] and lattice mismatch.[7] Fortunately, significant improvements in interfacial stability have been achieved by protective coating of the active materials with metal oxides such as $LiNbO_3$.[2a,d,5] Furthermore, wetting active materials with SEs is critical for high-performance bulk-type ASLBs.[2d,h,8] In the case of bulk-type ASLBs that employ oxide SE materials, high-temperature sintering processes are necessary to form contacts between active materials and SEs.[9] However, this can lead to the formation of undesirable byproducts at the interfaces, resulting in poor electrochemical performance.[9,10] In contrast, sulfide SEs are deformable, which allows efficient two-dimensional contact by simple cold-pressing,[2d,11] although full wetting of active materials with sulfide SEs by cold-pressing alone is still limited.[2d,h,8,11b,12]

A pioneering proof-of-concept for direct SE coating of active materials using pulsed laser deposition, and the resulting improvement in ASLB performance, has been reported.[13] The wet-chemical preparation of SEs could be one of the most appropriate strategies to realize the above-mentioned concept in a scalable way. However, the selection of effective combinations of SEs and solvents in which the SEs can be dissolved without irreversible chemical reaction with the solvents is extremely challenging.[2d,h,8,11b] To date, very few wet-chemical systems for the preparation of sulfide SEs have been reported. These include thio-LISICON ($Li_{3.25}Ge_{0.25}P_{0.75}S_4$, 0.182 mS cm^{-1}) and anhydrous hydrazine,[14] Li_3PS_4 and tetrahydrofuran (0.16 mS cm^{-1})[15] or *N*-methylformamide (0.026 mS cm^{-1}),[16] $Li_7P_2S_8I$ and acetonitrile (0.63 mS cm^{-1}),[17] and Li_6PS_5Cl and ethanol (0.014 mS cm^{-1}).[18] However, none of these systems simultaneously satisfy the multiple criteria required for a scalable solution-based SE-coating process, that is, high conductivity (at

[a] Y. E. Choi,[+] Dr. K. H. Park,[+] D. H. Kim, D. Y. Oh, H. R. Kwak, Prof. Y. S. Jung
School of Energy and Chemical Engineering
Department of Energy Engineering
Ulsan National Institute of Science and Technology (UNIST)
Ulsan 44919 (South Korea)
E-mail: ysjung@unist.ac.kr

[b] Dr. Y.-G. Lee
Power Control Device Research Team
Electronics and Telecommunications Research Institute (ETRI)
218 Gajeongno, Yuseong-gu, Daejeon 305-700 (South Korea)

[+] These authors contributed equally to this work.

Supporting Information and the ORCID identification number(s) for the author(s) of this article can be found under https://doi.org/10.1002/cssc.201700409.

least 0.1 mS cm^{-1}), environmental benignity, and the use of low-cost, low-boiling-point solvents that afford homogeneous solutions.

Another critical issue is that conventional sulfide SEs that contain phosphorus, such as Li_3PS_4 and $L_{10}GeP_2S_{12}$, undergo degradation upon exposure to water or dry air,[2d] as do phosphorus-containing Na-ion SEs such as Na_3PS_4.[12] However, recent reports of the excellent air-stability of Li_4SnS_4 (LSS),[2d,19] $Li_{4-x}Sn_{1-x}As_xS_4$,[20] and Li_2SnS_3[21] have led to interest in developing alternative Sn-based SEs. The superior dry-air stability of Sn-based SEs to that of phosphorus-based SEs has been explained by reference to the hard and soft acid and base theory.[2d,8,20]

Recently, our group reported a new, highly conductive, and dry-air-stable Sn-based Li-ion SE, 0.4LiI-0.6Li_4SnS_4 (0.41 mS cm^{-1}), prepared from a homogeneous MeOH solution.[2d] ASLBs employing $LiCoO_2$ coated with this SE exhibited excellent performance. Herein, our development of Sn-based SEs is expanded to a solution process for Li_4SnS_4 using the most environmentally desirable and nontoxic solvent (water), and its application for SE-coating of active materials for ASLBs.

Results and Discussion

The X-ray diffraction (XRD) pattern of crystalline Li_4SnS_4 (SS-LSS) (Figure 1a) matches well with that of orthorhombic Li_4SnS_4 with the space group *Pnma*.[19] The SS-LSS powder was dissolved in deionized water, forming a transparent greenish-yellow solution (Figure S1 in the Supporting Information). Figure 2a compares the amount of H_2S evolved from aqueous SE solutions for phosphorus-free LSS and phosphorus-containing $Li_{10}GeP_2S_{12}$. In contrast to the aggressive H_2S evolution for the $L_{10}GeP_2S_{12}$ solution, H_2S evolution was negligible for the LSS solution, which reflects the absence of side reactions and the intactness of SnS_4^{4-} in aqueous solution. Figure 2b shows the thermogravimetric analysis (TGA) profile of the solid $Li_4SnS_4{\cdot}xH_2O$ powder obtained from the solution by treatment under vacuum at room temperature. Weight loss is evident at around 150 °C; thus, heat-treatment temperatures of 200, 240, 280, 320, 360, 400, and 450 °C were selected to obtain the final samples. Hereafter, the aqueous-solution-processed samples of xLiI-(1−x)Li_4SnS_4 heat-treated at a given temperature of y (°C) are referred to as "xLiI-(1−x)LSSy".

Figure 1a displays the XRD patterns of the aqueous-solution-processed LSS samples heat-treated at different temperatures. The XRD patterns show amorphous features up to heat-treatment temperatures of 320 °C. Crystalline peaks appear for heat-treatment temperature above 320 °C without any noticeable impurity phases. Despite their distinct difference in XRD crystallinities, the Raman spectra of LSS450 and LSS320 both show strong peaks centered at 345 cm^{-1}, originating from SnS_4^{4-} (Figure S2).[2d] The ionic conductivities of the solution-processed LSS samples at 30 °C (Figure 1b) show a gradual increase as the heat-treatment temperature increases to 320 °C (LSS320), reaching the maximum value of 0.14 mS cm^{-1}. The conductivity of highly crystalline LSS450 is one order of magnitude lower (0.014 mS cm^{-1}), which agrees well with our previously reported results for MeOH-solution-processed LSS.[2d] Crystalline LSS450 may exhibit poorer deformability than the XRD-amorphous samples (e.g., LSS320), resulting in higher grain-boundary resistances in the cold-pressed pellet.[2d] Importantly, in line with previous reports,[2d,20,21] the aqeous-solution-processed LSS appears to be stable upon exposure to dry air. LSS320 shows a marginal decrease in conductivity after exposure to dry air for 24 h (0.11 mS cm^{-1}) (Figure S3).

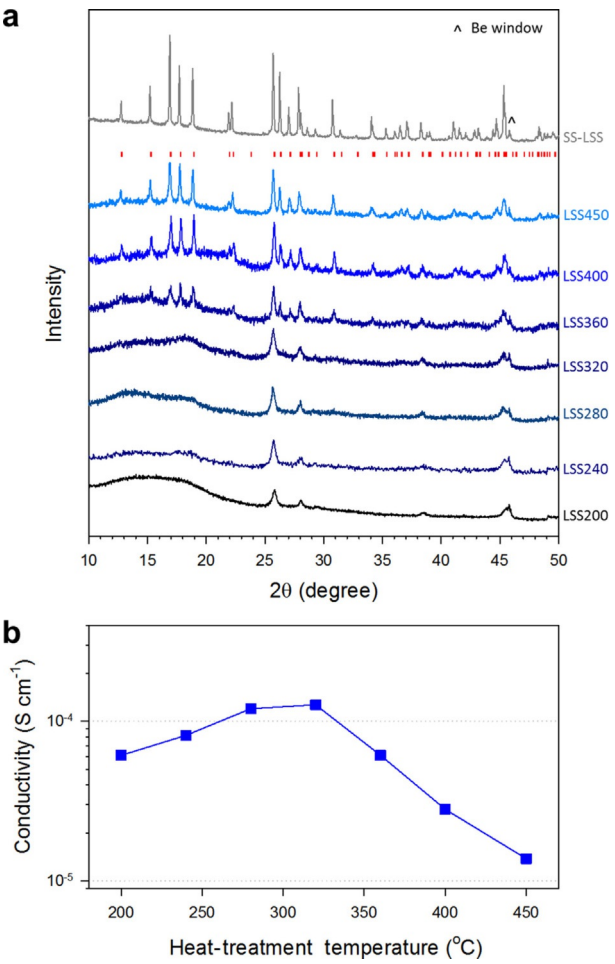

Figure 1. a) XRD patterns and b) ionic conductivities of aqueous-solution processed LSS at 30 °C as a function of heat-treatment temperature.

The aqueous-solution process was applied to SE-coating of the active material $LiCoO_2$. Figure 3 illustrates the process of SE-coating and its application to $LiCoO_2$/Li-In all-solid-state cells. Figure 4a shows a field-emission scanning electron microscopy (FESEM) image of an LSS-coated $LiCoO_2$ particle (15 wt% LSS) and its corresponding energy-dispersive X-ray spectroscopy (EDX) elemental maps, which indicate that the SE layers cover the $LiCoO_2$ particle well. The Raman spectrum of the LSS-coated $LiCoO_2$ powder is almost identical to that of LSS320 (Figure S4). High-resolution transmission electron microscopy (HRTEM) images and the corresponding EDX elemental maps of a focused ion beam (FIB)-cross-sectioned LSS-coated $LiCoO_2$ particle (Figure 4b and Figure S5) highlight the intimate contact between the LSS coating layer and the $LiCoO_2$. Contrary to the XRD-amorphous features of LSS320

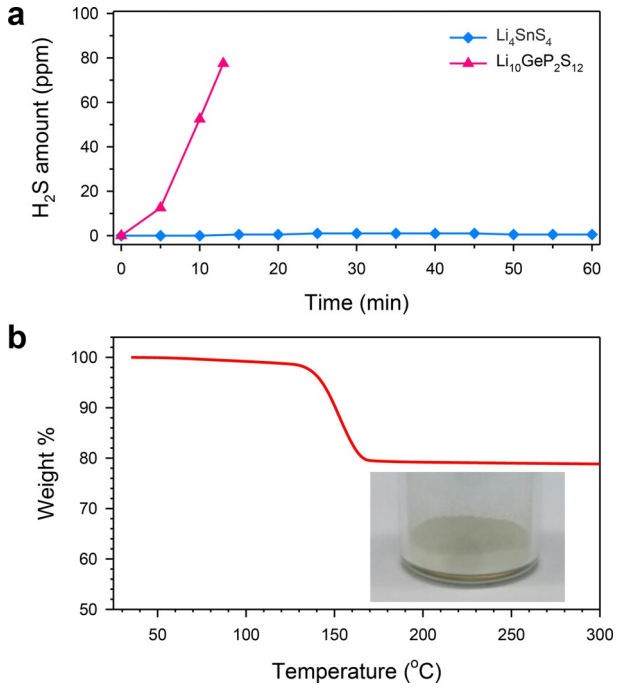

Figure 2. a) H_2S amount as a function of time for the aqueous SE solution. b) TGA profile of the powder obtained by drying the aqueous LSS solution under vacuum at room temperature. A photograph of the LSS powder prepared from aqueous solution with a heat-treatment temperature of 200 °C is shown in the inset.

(Figure 1a), the coated LSS layer exhibits glass-ceramic-like features with nanocrystallites (Figure S5), which is consistent with our previous results.[2d] The interlayer spacing values obtained from the lattice fringes correspond with those for LSS (Figure S5b).

The positive composite electrodes of $LiCoO_2$/Li-In all-solid-state cells were fabricated either by manually mixing $LiCoO_2$ and SE (LSS320) powders or by using LSS-coated $LiCoO_2$ powders. A bilayer SE, in which $L_{10}GeP_2S_{12}$ (6.0 mS cm^{-1}) and Li_3PS_4 (1.0 mS cm^{-1}) are in contact with the $LiCoO_2$ and Li-In electrodes, respectively, was employed to maximize the rate capability and avoid degradation of $L_{10}GeP_2S_{12}$ at low voltage.[2d,22] Two different LSS-coated $LiCoO_2$ powder samples were prepared, one by adding $LiCoO_2$ and LSS320 powders together in deionized water (referred to as "Coated 1") and one by adding $LiCoO_2$ powder to a predissolved LSS solution (referred to as "Coated 2"). For the former (Coated 1), direct exposure of some parts of $LiCoO_2$ to fresh water in short times would be inevitable. For fair comparison with the LSS-coated $LiCoO_2$, accordingly, two kinds of $LiCoO_2$ for the mixed electrodes were used; pristine $LiCoO_2$ (p-LCO) and water-treated $LiCoO_2$ (w-LCO). The w-LCO sample was prepared by immersing $LiCoO_2$ powders into deionized water overnight, followed by dehydration at 320 °C under vacuum.

The electrochemical performances of the mixed and coated electrodes are shown in Figure 5. Compared to the mixed electrode with p-LCO, the coated electrodes exhibit significant improvements in rate capability. The coated electrodes retain 64% capacity (79 mA h g^{-1}) for Coated 1 and 71% (97 mA h g^{-1}) for Coated 2 at 1C compared to 0.1C, which is in contrast to the 40% (54 mA h g^{-1}) for the mixed electrode with p-LCO. However, considering that the $LiCoO_2$ used for the coated elec-

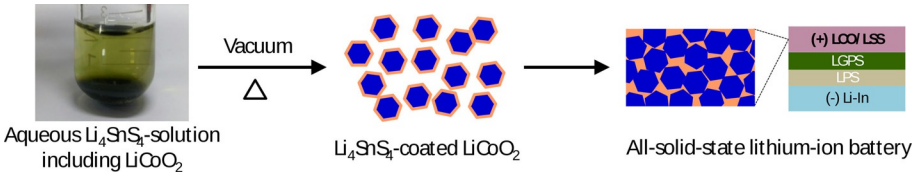

Figure 3. Schematic illustration of the aqueous-solution process for LSS-coated $LiCoO_2$ for ASLBs.

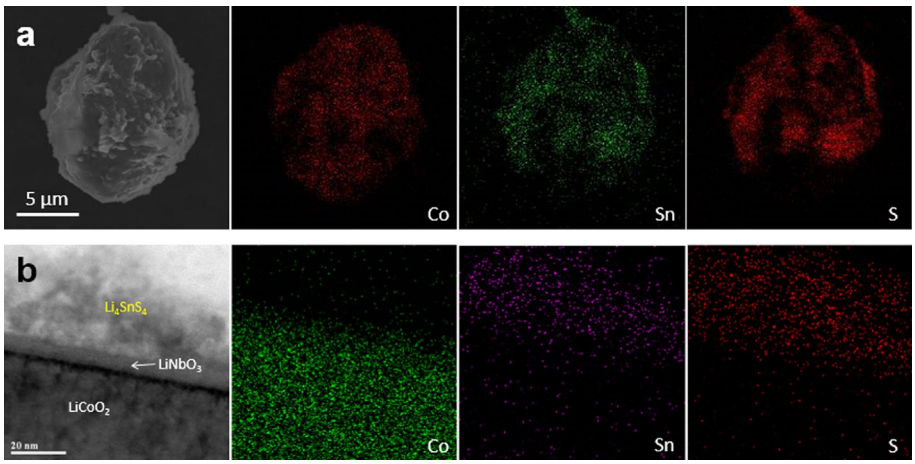

Figure 4. Electron microscopy images of LSS-coated $LiCoO_2$ particles obtained by the aqueous-solution process. a) FESEM image of an LSS-coated $LiCoO_2$ particle and its corresponding EDX elemental maps. b) HRTEM image of an FIB-cross-sectioned LSS-coated $LiCoO_2$ particle and its corresponding EDX elemental maps.

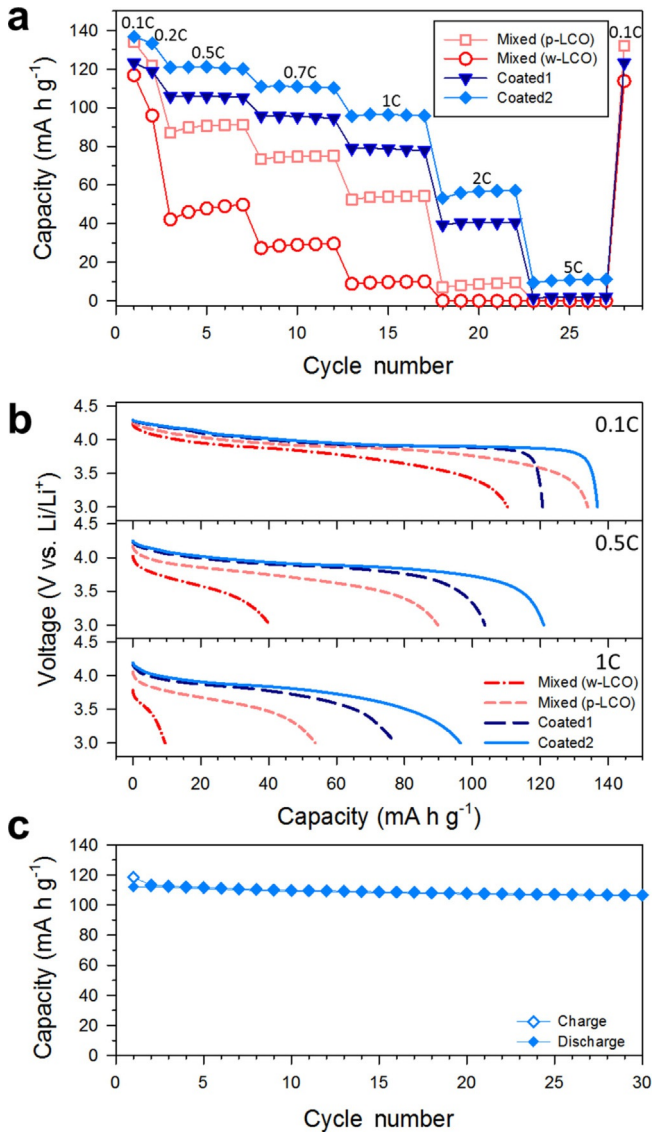

Figure 5. Electrochemical performances of the mixed electrodes and the LSS-coated $LiCoO_2$ electrodes cycled in a voltage range of 3.0–4.3 V (vs. Li/Li^+). a) Variation in discharge capacity versus charge–discharge cycle number at different C-rates. b) Discharge-voltage profiles at different C-rates. c) Cycle performance of the LSS-coated $LiCoO_2$ electrode (Coated 2). p-LCO and w-LCO indicates pristine and water-treated LCO, respectively. The $LiCoO_2$/LSS weight ratio in the composite electrodes was 85:15.

trodes was in contact with an aqueous environment during the solution process, a more relevant comparison can be made by comparing the results with those of the mixed electrode made by using w-LCO. The mixed electrode made with w-LCO shows a significantly poorer rate capability than the mixed electrode made by using p-LCO, implying the detrimental effect of exposure to water. It is known that surface impurities such as Li_2O, LiOH, and Li_2CO_3 are formed if $LiMO_2$ (M = Co, Ni, Mn) materials are exposed to water or ambient air.[23] The severe degradation in rate capability of the mixed electrode made with w-LCO compared to that with p-LCO is thus explained by contamination of the surfaces.[23c] This observation also agrees with the degradation in rate capability of $LiCoO_2$ upon exposure for conventional LIB cells using liquid electrolytes (Figure S6).

Surface analysis for $LiCoO_2$ powders before and after exposure to deionized water or aqueous LSS solution was performed by X-ray photoelectron spectroscopy (XPS) (Figure 6)

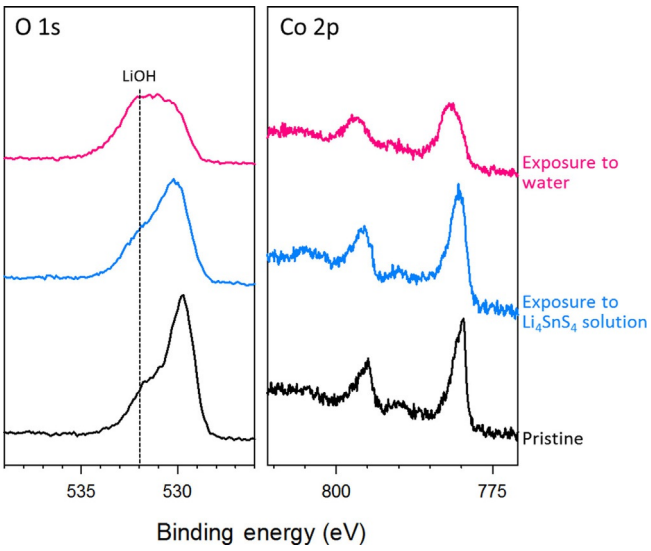

Figure 6. XPS spectra of $LiCoO_2$ powders before and after exposure to water or LSS solution. The signals for O 1s and Co 2p are shown.

and time-of-flight secondary ion mass spectrometry (TOFSIMS) (Figure S7). The O 1s XPS spectrum for the pristine $LiCoO_2$ exhibits two distinct peaks; the sharp peak at approximately 530 eV and the satellite peak at approximately 532 eV, which are attributed to $LiCoO_2$ and impurities such as LiOH, respectively (see Table S1 for the detailed peak positions). After exposure to LSS solution, changes to the overall XPS spectra are marginal. In stark contrast, the O 1s XPS spectrum for the water-exposed $LiCoO_2$ shows a remarkably increased intensity for the LiOH peak. This observation is in line with the stronger $LiOH^+$ signal for the water-exposed $LiCoO_2$ than for the LSS-solution-exposed $LiCoO_2$ in TOFSIMS spectra (Figure S7). Considering that the surface degradation of $LiCoO_2$ upon exposure to water is related to the activity of protons, the high basicity of the aqueous LSS solution (pH 11.89) would be effective to minimize surface contamination.[23c] This explains the slightly better rate performance for Coated 2 than that for Coated 1; the side reactions at the surface of $LiCoO_2$ are less severe in the predissolved LSS solution than in water. Overall, considering this negative effect of the exposure of $LiCoO_2$ to aqueous solutions, the superior rate capability of the aqueous-solution-processed LSS-coated $LiCoO_2$ electrode to that of the mixed electrode made with p-LCO demonstrates the importance of ionic contact between SE and active materials in ASLBs.[2d,12] It is believed that the development of a functional protective coating to minimize side reactions occurring in aqueous solution can further improve the performance,[24] and that adopting alternative electrode materials that are compatible with aqueous environments[25] can leverage the advantage of aqueous-solution-processable Sn-based SEs, which will be the sub-

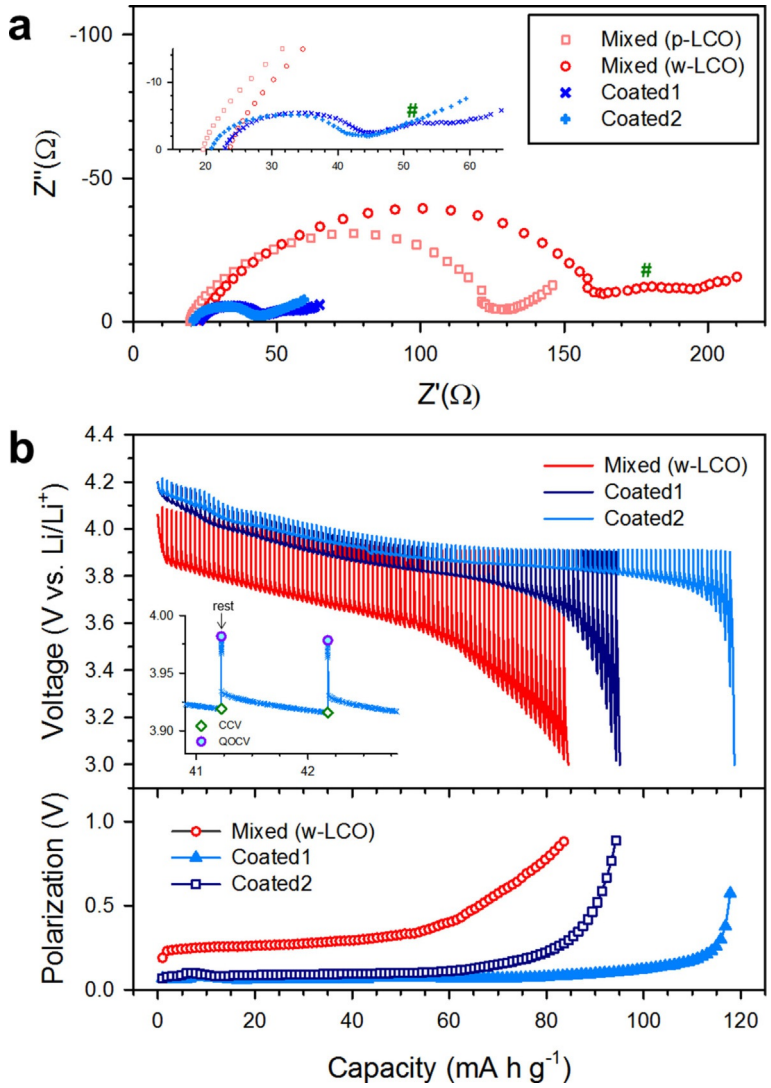

Figure 7. Electrochemical characterization of the mixed electrodes and the LSS-coated $LiCoO_2$ electrodes. a) Nyquist plots and b) discharge-voltage profiles and their corresponding polarization plots obtained by GITT. A magnified view of the Nyquist plots is shown in the inset of a). An enlarged view of the transient voltage profile for Coated 2 is shown in the inset of b). The polarization curves in b) were plotted by subtracting the closed-circuit voltage (CCV) from the quasi-open-circuit voltage (QOCV) in the transient voltage profiles.

jects of our next studies. As shown in Figure 5c, the Coated 2 electrode cycled in the voltage range of 3.0–4.3 V (vs. Li/Li^+) at 0.5 C exhibits stable cycling performance.

Consistent with the trend of rate capability illustrated in Figure 5a, the discharge voltage profiles at different C-rates indicate higher polarization in the order of the mixed electrode made using w-LCO, the mixed electrode made using p-LCO, and the coated electrodes (Figure 5b). In an attempt to deconvolute the contributions to the overall rate capabilities, the Nyquist plots were compared (Figure 7a). The spectra show one or more semicircles at higher frequency, followed by the Warburg tails at lower frequency. The intercept at the *x* axis is assigned to the resistance of $L_{10}GeP_2S_{12}/Li_3PS_4$ bilayer SE.[2d] The semicircles are interpreted as being a result of the contributions of interfacial charge-transfer and electronic resistances.[2d,h,22,26] The order of the overall amplitude of the semicircles in Figure 7a (ca. 180 Ω for the w-LCO-mixed electrode, ca. 110 Ω for the p-LCO-mixed electrode, ca. 20 Ω for the coated electrodes) agrees perfectly with the results for rate capability (Figure 5a, b). The evolution of mid-frequency semicircles denoted as '#' for the mixed electrode made with w-LCO and for the Coated 1 electrode is assigned to contribution by the surface impurities formed in aqueous environments. The absence of a mid-frequency semicircle for Coated 2 confirms the superior stability of $LiCoO_2$ in the predissolved LSS solution to that in water. Most importantly, it should be noted that the amplitude of the semicircles is also dependent on the interfacial contact area between active materials and SEs. Thus, the much smaller semicircles for the coated electrodes than those for the mixed electrodes imply intimate ionic contact. Figure 7b compares the GITT (galvanostatic intermittent titration technique) voltage profiles for the mixed electrode made with w-LCO and the LSS-coated $LiCoO_2$ electrodes (Coated 1 and Coated 2), and their corresponding polarization plots, which

again confirms the dramatic improvement by direct SE coating of the active material. The interfacial contact areas between the SE and $LiCoO_2$ were also derived from the GITT curves,[2d,h,27] and they are much higher for the coated electrode (Coated 1, 50%) than for the mixed electrode (23%). Additionally, consistent with the results of rate capability (Figure 5a, b) and electrochemical impedance spectroscopy (EIS) (Figure 7a), the lower polarization for the Coated 2 electrode than for Coated 1 is confirmed by the GITT result (Figure 7b).

LiI·LSS were also prepared by the aqueous-solution process. In contrast to previously reported MeOH-solution processed LiI·LSS, characteristic peaks attributed to LiI (JCPDS no. 71-3746) were observed (Figure S8a).[2d] This discrepancy emphasizes the role of the solvent in solution chemistry in terms of nucleation and growth of crystals.[28] It is interesting that, despite the observation of segregated crystalline LSS and LiI, the ionic conductivities of LiI·LSS prepared at 200 °C are higher than that of the LiI-free sample (Figure S8b). However, the rate capability of LiI·LSS-coated $LiCoO_2$ was inferior to LSS-coated $LiCoO_2$ (Figure S9). Considering the almost identical conductivity value of 0.4LiI·0.6LSS heat-treated at 200 °C (0.10 mS cm^{-1}) and LSS (0.14 mS cm^{-1}) by 320 °C heat treatment, the distinct difference in rate capability might originate from the presence of I^- ions. It is expected that the segregated LiI decomposes at high voltage, thus negatively affecting the interfaces.[29] Care should be taken, however, when comparing these results with the previously reported MeOH-solution processed LiI·LSS, because it did not form segregated LiI.[2d] It is thought that the electrochemical stability of the I^- ions in the MeOH-solution processed LiI·LSS and pure LiI would be different.

Conclusions

A highly conductive, dry-air-stable, and coatable solid electrolyte (SE), Li_4SnS_4 (LSS), was successfully prepared by a scalable aqueous-solution process. The highest ionic conductivity of 0.14 mS cm^{-1} was achieved for the aqueous-solution-processed LSS heat-treated at 320 °C. The all-solid-state lithium-ion batteries (ASLBs) employing the LSS-coated $LiCoO_2$ significantly outperformed the conventional mixed electrodes, highlighting the critical importance of intimate ionic contact. The negative effect on interfaces caused by the exposure of $LiCoO_2$ to aqueous solutions was alleviated by using a predissolved LSS solution. We believe that these results are of importance to the commercialization of high-performance all-solid-state technologies.

Experimental Section

Preparation of materials

Crystalline LSS powders as precursors for the aqueous-solution process were prepared by conventional solid-state synthesis and denoted "SS-LSS". A stoichiometric mixture of Li_2S (99.9%, Alfa Aesar), elemental tin (99.8%, Alfa Aesar), and elemental sulfur (99.5%, Alfa Aesar) was heat-treated at 650 °C for 24 h in a quartz ampoule sealed under vacuum. After the LSS powders were dissolved in deionized water, undissolved impurities were removed by filtration. After the filtered solution was subjected to vacuum and the subsequent heat-treatment at designated temperatures under vacuum, the final powder samples were obtained. The $L_{10}GeP_2S_{12}$ powders were prepared by solid-state reaction of a stoichiometric mixture of Li_2S, P_2S_5, and GeS_2 (99.9%, American Elements) at 550 °C for 12 h in a quartz ampoule sealed under vacuum, as described in our previous reports.[2d,8,22] The aqueous LSS (LSS320) or $L_{10}GeP_2S_{12}$ solutions for measurement of the H_2S amount were prepared by dissolving SE powders (100 mg) in deionized water (1 mL). The solutions were kept in a closed container (2.5 L) in which an air was circulated by a small electric fan. The amount of H_2S was measured using an H_2S sensor (SP2297, SENKO). The LSS-coated $LiCoO_2$ powders were prepared by the same aqueous-solution process in the presence of $LiCoO_2$ powders with heat-treatment temperatures of 320 and 200 °C, respectively (Figure 3). The $LiNbO_3$-coated $LiCoO_2$ powders were used for the LSS coating.[2d,11b] Li_3PS_4 powders were prepared by a mechanochemical method. A stoichiometric mixture of Li_2S and P_2S_5 (99%, Sigma–Aldrich) was ball-milled at 500 rpm for 10 h and subsequently heat-treated at 243 °C for 1 h in a glass ampoule sealed under vacuum.[2d]

Materials characterization

The TGA experiment was conducted from 30 to 300 °C at 5 °C min^{-1} on a SDT Q600 (TA Instrument Corp.) under Ar flow. For XRD measurements, samples were loaded onto the XRD holder and sealed under beryllium window for inhibition of air exposure. A D8-Bruker Advance Diffractometer (CuKα radiation, 1.54056 Å) was used at 40 kV and 40 mA at 15° min^{-1}. FESEM images and the corresponding EDX elemental maps were obtained using a S-4800 (Hitachi Corp.). HRTEM images and the corresponding EDX elemental maps were obtained using a JEM-2100 (JEOL). The elemental composition of aqueous-solution processed SEs and the weight fraction of SEs coated on $LiCoO_2$ were determined by inductively coupled plasma optical emission spectroscopy (ICP-OES) on a 720-ES (Varian Corp.). For the dry-air-stability test, SE powder (100 mg) was kept under a flow of dry air (a mixture of 21:79 *v*/*v*) for 24 h. For the surface analysis by XPS and TOFSIMS, $LiCoO_2$ powders exposed to water or LSS solution were prepared. After exposure to the liquids, the samples were rinsed with anhydrous MeOH several times, followed by drying under vacuum at 320 °C. XPS measurements were performed using a K-alpha X-ray photoelectron spectrometer (Thermo Fisher) with a monochromatic AlKα source (1486.6 eV). TOFSIMS analyses were conducted on a TOF SIMS 5 (ION TOF). A 25 kV Bi^+ source was employed for analysis.

All-solid-state cells

Composite electrodes were prepared from the $LiCoO_2$/LSS mixture electrode or the LSS-coated $LiCoO_2$. The weight ratio of $LiCoO_2$/SE was 85:15. All-solid-state cells were fabricated in a 13 mm diameter polyaryletheretherketone mold. After a $L_{10}GeP_2S_{12}/Li_3PS_4$ bilayer film consisting of $L_{10}GeP_2S_{12}$ (120 mg) and Li_3PS_4 (30 mg) powders was formed by pelletizing, the composite electrode (15 mg) was put on the $L_{10}GeP_2S_{12}$ side and spread evenly. Then, $Li_{0.5}In$ (100 mg), which was prepared by mixing In (99%, Sigma–Aldrich) and Li (FMC Lithium Corp.) powders, was spread on the Li_3PS_4 side of the $L_{10}GeP_2S_{12}/Li_3PS_4$ bilayer. Finally, the cell was pressed at 370 MPa. The galvanostatic charge–discharge cycling of the all-solid-state cells was performed in a voltage range of 3.0–4.3 V (vs. Li/Li^+) at 30 °C. The EIS measurements were performed from 1.5 MHz to 5 mHz with an amplitude of 10 mV, using the cells charged to 30 mA h g^{-1} at 0.1 C and rested for more than 3 h. 1 C-

rate corresponds with 1.1 mA cm^{-2}. The GITT measurements were performed with the pulse of 0.5 C for 60 s and rest for 2 h.

Acknowledgements

This work was supported by the Energy Efficiency & Resources Program of the Korea Institute of Energy Technology Evaluation and Planning (KETEP) grant funded by the Korea government Ministry of Trade, Industry & Energy (No. 20152010103470) and by Basic Science Research Program through the National Research Foundation of Korea (NRF) funded by the Ministry of Education (No. NRF-2014R1A1A2058760).

Conflict of interest

The authors declare no conflict of interest.

Keywords: batteries · conductivity · solid electrolytes · solution processes · sulfides

[1] a) J. B. Goodenough, Y. Kim, *Chem. Mater.* **2010**, *22*, 587 – 603; b) A. Manthiram, X. Yu, S. Wang, *Nat. Rev. Mater.* **2017**, *2*, 16103.

[2] a) N. Kamaya, K. Homma, Y. Yamakawa, M. Hirayama, R. Kanno, M. Yonemura, T. Kamiyama, Y. Kato, S. Hama, K. Kawamoto, A. Mitsui, *Nat. Mater.* **2011**, *10*, 682 – 686; b) Y. S. Jung, D. Y. Oh, Y. J. Nam, K. H. Park, *Isr. J. Chem.* **2015**, *55*, 472 – 485; c) J. Janek, W. G. Zeier, *Nat. Energy* **2016**, *1*, 16141; d) K. H. Park, D. Y. Oh, Y. E. Choi, Y. J. Nam, L. L. Han, J. Y. Kim, H. L. Xin, F. Lin, S. M. Oh, Y. S. Jung, *Adv. Mater.* **2016**, *28*, 1874 – 1883; e) Y. Kato, S. Hori, T. Saito, K. Suzuki, M. Hirayama, A. Mitsui, M. Yonemura, H. Iba, R. Kanno, *Nat. Energy* **2016**, *1*, 16030; f) Y. Wang, W. D. Richards, S. P. Ong, L. J. Miara, J. C. Kim, Y. Mo, G. Ceder, *Nat. Mater.* **2015**, *14*, 1026 – 1031; g) T. A. Yersak, C. Stoldt, S. H. Lee, *J. Electrochem. Soc.* **2013**, *160*, A1009 – A1015; h) D. H. Kim, D. Y. Oh, K. H. Park, Y. E. Choi, Y. J. Nam, H. A. Lee, S.-M. Lee, Y. S. Jung, *Nano Lett.* **2017**, *17*, 3013 – 3020.

[3] a) Y. Seino, T. Ota, K. Takada, A. Hayashi, M. Tatsumisago, *Energy Environ. Sci.* **2014**, *7*, 627 – 631; b) T. Yamada, S. Ito, R. Omoda, T. Watanabe, Y. Aihara, M. Agostini, U. Ulissi, J. Hassoun, B. Scrosati, *J. Electrochem. Soc.* **2015**, *162*, A646 – A651.

[4] K. Xu, *Chem. Rev.* **2004**, *104*, 4303 – 4417.

[5] A. Sakuda, A. Hayashi, M. Tatsumisago, *Chem. Mater.* **2010**, *22*, 949 – 956.

[6] S. Wenzel, S. Randau, T. Leichtweiβ, D. A. Weber, J. Sann, W. G. Zeier, J. R. Janek, *Chem. Mater.* **2016**, *28*, 2400 – 2407.

[7] J. Haruyama, K. Sodeyama, L. Y. Han, K. Takada, Y. Tateyama, *Chem. Mater.* **2014**, *26*, 4248 – 4255.

[8] D. Y. Oh, Y. J. Nam, K. H. Park, S. H. Jung, S. J. Cho, Y. K. Kim, Y. G. Lee, S. Y. Lee, Y. S. Jung, *Adv. Energy Mater.* **2015**, *5*, 7.

[9] S. Ohta, J. Seki, Y. Yagi, Y. Kihira, T. Tani, T. Asaoka, *J. Power Sources* **2014**, *265*, 40 – 44.

[10] a) S. K. Jeong, M. Inaba, Y. Iriyarna, T. Abe, Z. Ogumi, *J. Power Sources* **2008**, *175*, 540 – 546; b) M. Kotobuki, H. Munakata, K. Kanamura, Y. Sato, T. Yoshida, *J. Electrochem. Soc.* **2010**, *157*, A1076 – A1079.

[11] a) A. Sakuda, A. Hayashi, M. Tatsumisago, *Sci. Rep.* **2013**, *3*, 2261; b) Y. J. Nam, S. J. Cho, D. Y. Oh, J. M. Lim, S. Y. Kim, J. H. Song, Y. G. Lee, S. Y. Lee, Y. S. Jung, *Nano Lett.* **2015**, *15*, 3317 – 3323.

[12] A. Banerjee, K. H. Park, J. W. Heo, Y. J. Nam, C. K. Moon, S. M. Oh, S.-T. Hong, Y. S. Jung, *Angew. Chem. Int. Ed.* **2016**, *55*, 9634 – 9638; *Angew. Chem.* **2016**, *128*, 9786 – 9790.

[13] A. Sakuda, A. Hayashi, T. Ohtomo, S. Hama, M. Tatsumisago, *Electrochem. Solid-State Lett.* **2010**, *13*, A73 – A75.

[14] Y. M. Wang, Z. Q. Liu, X. L. Zhu, Y. F. Tang, F. Q. Huang, *J. Power Sources* **2013**, *224*, 225 – 229.

[15] Z. C. Liu, W. J. Fu, E. A. Payzant, X. Yu, Z. L. Wu, N. J. Dudney, J. Kiggans, K. L. Hong, A. J. Rondinone, C. D. Liang, *J. Am. Chem. Soc.* **2013**, *135*, 975 – 978.

[16] S. Teragawa, K. Aso, K. Tadanaga, A. Hayashi, M. Tatsumisago, *J. Power Sources* **2014**, *248*, 939 – 942.

[17] E. Rangasamy, Z. C. Liu, M. Gobet, K. Pilar, G. Sahu, W. Zhou, H. Wu, S. Greenbaum, C. D. Liang, *J. Am. Chem. Soc.* **2015**, *137*, 1384 – 1387.

[18] S. Yubuchi, S. Teragawa, K. Aso, K. Tadanaga, A. Hayashi, M. Tatsumisago, *J. Power Sources* **2015**, *293*, 941 – 945.

[19] T. Kaib, S. Haddadpour, M. Kapitein, P. Bron, C. Schroder, H. Eckert, B. Roling, S. Dehnen, *Chem. Mater.* **2012**, *24*, 2211 – 2219.

[20] G. Sahu, Z. Lin, J. C. Li, Z. C. Liu, N. Dudney, C. D. Liang, *Energy Environ. Sci.* **2014**, *7*, 1053 – 1058.

[21] J. A. Brant, D. M. Massi, N. A. W. Holzwarth, J. H. MacNeil, A. P. Douvalis, T. Bakas, S. W. Martin, M. D. Gross, J. A. Aitken, *Chem. Mater.* **2015**, *27*, 189 – 196.

[22] B. R. Shin, Y. J. Nam, D. Y. Oh, D. H. Kim, J. W. Kim, Y. S. Jung, *Electrochim. Acta* **2014**, *146*, 395 – 402.

[23] a) H. S. Liu, Z. R. Zhang, Z. L. Gong, Y. Yang, *Electrochem. Solid-State Lett.* **2004**, *7*, A190 – A193; b) Z. H. Chen, J. R. Dahn, *Electrochem. Solid-State Lett.* **2003**, *6*, A221 – A224; c) M. Motzko, M. A. C. Solano, W. Jaegermann, R. Hausbrand, *J. Phys. Chem. C* **2015**, *119*, 23407 – 23412.

[24] a) Y. S. Jung, P. Lu, A. S. Cavanagh, C. Ban, G. H. Kim, S. H. Lee, S. M. George, S. J. Harris, A. C. Dillon, *Adv. Energy Mater.* **2013**, *3*, 213 – 219; b) A. Tron, Y. D. Park, J. Mun, *J. Power Sources* **2016**, *325*, 360 – 364.

[25] H. Kim, J. Hong, K. Y. Park, H. Kim, S. W. Kim, K. Kang, *Chem. Rev.* **2014**, *114*, 11788 – 11827.

[26] a) A. J. Bard, L. R. Faulkner, J. Leddy, C. G. Zoski in *Electrochemical methods: fundamentals and applications*, John Wiley & Sons, New York, **1980**; b) E. Kang, Y. S. Jung, G. H. Kim, J. Chun, U. Wiesner, A. C. Dillon, J. K. Kim, J. Lee, *Adv. Funct. Mater.* **2011**, *21*, 4349 – 4357; c) M. Gaberscek, J. Moskon, B. Erjavec, R. Dominko, J. Jamnik, *Electrochem. Solid-State Lett.* **2008**, *11*, A170 – A174.

[27] W. Weppner, R. A. Huggins, *J. Electrochem. Soc.* **1977**, *124*, 1569 – 1578.

[28] M. Mucha, P. Jungwirth, *J. Phys. Chem. B* **2003**, *107*, 8271 – 8274.

[29] H. D. Lim, H. Song, J. Kim, H. Gwon, Y. Bae, K. Y. Park, J. Hong, H. Kim, T. Kim, Y. H. Kim, X. Lepro, R. Ovalle-Robles, R. H. Baughman, K. Kang, *Angew. Chem. Int. Ed.* **2014**, *53*, 3926 – 3931; *Angew. Chem.* **2014**, *126*, 4007 – 4012.

Manuscript received: March 6, 2017
Revised manuscript received: May 7, 2017
Accepted manuscript online: May 8, 2017
Version of record online: May 31, 2017